Solution of the Laplace equation in 3D by multidomain BEM

Jure Ravnik, Leopold Škerget, Zoran Žunič

June 16, 2007

Abstract

This technical note describes the solution of the Laplace Equation by the Boundary Element Method applied to each mesh element.

1 Introduction

In order to avoid full matrices of integral values we use the multi-domain BEM approach. We write the BEM equation for each mesh element separately.

2 Numerical method

The main aspects of the implementation of the numerical method are shown below.

2.1 Boundary integral equation

The Laplace equation for a scalar field function $u(\vec{r})$, $\vec{r} \in \mathbb{R}^3$ is

$$\nabla^2 u(\vec{r}) = 0. \tag{1}$$

We seek a solution for u in a domain $\Omega \in \mathbb{R}^3$ with a boundary $\Gamma \in \mathbb{R}^2$ with function on the boundary

$$u(\vec{r}), \qquad \vec{r} \in \Gamma \tag{2}$$

or flux on the boundary

$$q(\vec{r}) = \nabla u(\vec{r}) \cdot \vec{n}, \qquad \vec{r} \in \Gamma \tag{3}$$

are prescribed as boundary conditions. Outward pointing normal to the boundary is denoted by $\vec{n}$.

Boundary integral representation of the Laplace equation (Wrobel [2], Ravnik [1]) is

$$c(\vec{\vartheta})u(\vec{\vartheta}) + \int_\Gamma u(\vec{r})\vec{\nabla}u^\star(\vec{\vartheta},\vec{r}) \cdot d\vec{\Gamma} = \int_\Gamma u^\star(\vec{\vartheta},\vec{r})\vec{\nabla}u(\vec{r}) \cdot d\vec{\Gamma} \qquad \vec{\vartheta} \in \Gamma, \tag{4}$$

where $\vec{\vartheta}$ is the source point. $c(\vec{\vartheta})$ is the geometric factor defined as

$$c(\vec{\vartheta}) = \int_0^\alpha \frac{d\theta}{4\pi} = \frac{\alpha}{4\pi}, \tag{5}$$

where α is the inner angle with origin in $\vec{\vartheta}$. If $\vec{\vartheta}$ lies inside of the domain than $c(\vec{\vartheta}) = 1$; $c(\vec{\vartheta}) = 1/2$, if $\vec{\vartheta}$ lies on a smooth boundary. Fundamental solution of the Laplace equation in $3D$ is

$$u^\star(\vec{\vartheta}, \vec{r}) = \frac{1}{4\pi r}, \tag{6}$$

where $r = |\vec{\vartheta} - \vec{r}|$.

Using boundary normals, equation (4) may be rewritten by

$$c(\vec{\vartheta})u(\vec{\vartheta}) + \int_\Gamma u(\vec{r})\vec{\nabla}u^\star(\vec{\vartheta}, \vec{r}) \cdot \vec{n}d\Gamma = \int_\Gamma u^\star(\vec{\vartheta}, \vec{r})\vec{\nabla}u(\vec{r}) \cdot \vec{n}d\Gamma \qquad \vec{\vartheta} \in \Gamma, \tag{7}$$

Taking into account the definition of boundary flux in equation (3) we may furter simplify (7)

$$c(\vec{\vartheta})u(\vec{\vartheta}) + \int_\Gamma u(\vec{r})\vec{\nabla}u^\star(\vec{\vartheta}, \vec{r}) \cdot \vec{n}d\Gamma = \int_\Gamma u^\star(\vec{\vartheta}, \vec{r})q(\vec{r})d\Gamma \qquad \vec{\vartheta} \in \Gamma, \tag{8}$$

The integral on the left hand side of (8) may be rewritten using the expression for the fundamental solution (6)

$$u(\vec{r})\vec{\nabla}u^\star(\vec{\vartheta}, \vec{r}) \cdot \vec{n} = \frac{(\vartheta_x - x)n_x + (\vartheta_y - y)n_y + (\vartheta_y - y)n_y}{4\pi r^3}, \tag{9}$$

where $\vec{r} = (x, y, z)$, $\vec{\vartheta} = \vartheta_x, \vartheta_y, \vartheta_z)$ and $\vec{n} = (n_x, n_y, n_z)$ and

$$r = \sqrt{(\vartheta_x - x)^2 + (\vartheta_y - y)^2 + (\vartheta_y - y)^2}. \tag{10}$$

2.2 Discretization

In the macro element BEM numerical method, we will solve equation (8) for each mesh element. We chose hexahedron with quadratic interpolation for function and linear interpolation for flux. Interpolation of function and flux on each side of the hexahedron is done using a local coordinate system (ξ, η). Node distribution is shown on Figure 2

$$u(\xi, \eta) = \sum_{i=1}^{9} \varphi_i u_i \qquad q(\xi, \eta) = \sum_{i=1}^{4} \phi_i q_i \tag{11}$$

Interpolation functions for function

$$\begin{aligned}
\varphi_1 &= \frac{1}{4}(\xi - \xi^2)(\eta - \eta^2), & \varphi_2 &= \frac{1}{2}(1 - \xi^2)(\eta^2 - \eta), \\
\varphi_3 &= \frac{1}{4}(\xi + \xi^2)(\eta^2 - \eta), & \varphi_4 &= \frac{1}{2}(\xi + \xi^2)(1 - \eta^2), \\
\varphi_5 &= \frac{1}{4}(\xi + \xi^2)(\eta + \eta^2), & \varphi_6 &= \frac{1}{2}(1 - \xi^2)(\eta^2 + \eta), \\
\varphi_7 &= \frac{1}{4}(\xi^2 - \xi)(\eta + \eta^2), & \varphi_8 &= \frac{1}{2}(\xi - \xi^2)(\eta^2 - 1), \\
& & \varphi_9 &= (1 - \xi^2)(1 - \eta^2)
\end{aligned} \tag{12}$$

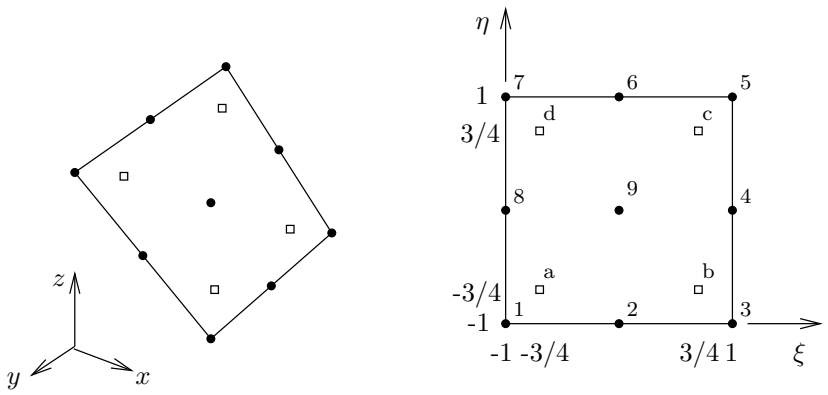

Figure 1: Linear interpolation for flux (squares) and quadratic interpolation for function (circles) over a surface. Left $\mathbb{R}^3$ space, right local coordinate system

and for flux

$$\begin{aligned} \phi_1 &= \frac{4}{9}(\xi - \frac{3}{4})(\eta - \frac{3}{4}), \qquad \phi_2 = -\frac{4}{9}(\xi + \frac{3}{4})(\eta - \frac{3}{4}), \\ \phi_3 &= \frac{4}{9}(\xi + \frac{3}{4})(\eta + \frac{3}{4}), \qquad \phi_4 = -\frac{4}{9}(\xi - \frac{3}{4})(\eta + \frac{3}{4}). \end{aligned} \tag{13}$$

. The geometry of the hexahedron is defined by 8 corner nodes, thus each surface is defined by 4 nodes (numbers 1,3,5,7 in Figure 2). One may find the location of flux nodes (a,b,c,d) by the following transformation

$$\begin{vmatrix} x_a & y_a & z_a \\ x_b & y_b & z_b \\ x_c & y_c & z_c \\ x_d & y_d & z_d \end{vmatrix} = \frac{1}{64} \begin{vmatrix} 49 & 7 & 1 & 7 \\ 7 & 49 & 7 & 1 \\ 1 & 7 & 49 & 7 \\ 7 & 1 & 7 & 49 \end{vmatrix} \cdot \begin{vmatrix} x_1 & y_1 & z_1 \\ x_3 & y_3 & z_3 \\ x_5 & y_5 & z_5 \\ x_7 & y_7 & z_7 \end{vmatrix} \tag{14}$$

Due to the fact, that the surface is defined by four nodes only, we may interpolate a location of the surface by

$$x(\xi,\eta) = \sum_{i=1}^{4} \Phi_i x_i, \qquad y(\xi,\eta) = \sum_{i=1}^{4} \Phi_i y_i, \qquad z(\xi,\eta) = \sum_{i=1}^{4} \Phi_i z_i, \tag{15}$$

where

$$\begin{aligned} \Phi_1 &= \frac{1}{4}(\xi - 1)(\eta - 1), \qquad \Phi_2 = -\frac{1}{4}(\xi + 1)(\eta - 1), \\ \Phi_3 &= \frac{1}{4}(\xi + 1)(\eta + 1), \qquad \Phi_4 = -\frac{1}{4}(\xi - 1)(\eta + 1). \end{aligned} \tag{16}$$

Having interpolation in mind, we may rewrite the integral equation (8)

$$c(\vec{\vartheta})u(\vec{\vartheta}) + \sum_{i=1}^{9} u_i \int_\Gamma \varphi_i \vec{\nabla} u^\star(\vec{\vartheta},\vec{r}) \cdot \vec{n} d\Gamma = \sum_{i=1}^{4} q_i \int_\Gamma \phi_i u^\star(\vec{\vartheta},\vec{r}) q(\vec{r}) d\Gamma. \tag{17}$$

The integrals are traditionally named

$$c(\vec{\vartheta})u(\vec{\vartheta})H^i_{\vartheta,\Gamma} = \int_\Gamma \varphi_i \vec{\nabla} u^\star(\vec{\vartheta},\vec{r})\cdot\vec{n}d\Gamma, \qquad G^i_{\vartheta,\Gamma} = \int_\Gamma \phi_i u^\star(\vec{\vartheta},\vec{r})q(\vec{r})d\Gamma \tag{18}$$

thus the discrete equation is

$$c(\vec{\vartheta})u(\vec{\vartheta}) + \sum_{i=1}^{9} u_i H^i_{\vartheta,\Gamma} = \sum_{i=1}^{4} q_i G^i_{\vartheta,\Gamma}. \tag{19}$$

2.3 Integration

A Gaussian quadrature algorithm will be used, thus the integrals must be written in local coordinate system (ξ,η):

$$H^i_{\vartheta,\Gamma} = \int_\Gamma \varphi_i \frac{(\vartheta_x - \sum_{j=1}^4 \Phi_j x_j)n_x + (\vartheta_y - \sum_{j=1}^4 \Phi_j y_j)n_y + (\vartheta_z - \sum_{j=1}^4 \Phi_j z_j)n_z}{4\pi[(\vartheta_x - \sum_{j=1}^4 \Phi_j x_j)^2 + (\vartheta_y - \sum_{j=1}^4 \Phi_j y_j)^2 + (\vartheta_z - \sum_{j=1}^4 \Phi_j z_j)^2]^{3/2}} d\Gamma \tag{20}$$

$$G^i_{\vartheta,\Gamma} = \int_\Gamma \phi_i \frac{1}{4\pi[(\vartheta_x - \sum_{j=1}^4 \Phi_j x_j)^2 + (\vartheta_y - \sum_{j=1}^4 \Phi_j y_j)^2 + (\vartheta_z - \sum_{j=1}^4 \Phi_j z_j)^2]^{1/2}} d\Gamma, \tag{21}$$

where interpolation functions φ, ϕ, Φ are all functions of (ξ,η) and $\vartheta_x, \vartheta_x, \vartheta_x, x_j, y_j, z_j$ are known locations of the mesh. Surface element $d\Gamma$ is transformed

$$d\Gamma = |J| d\xi d\eta, \tag{22}$$

where $|J|$ is the Jacobian determinant defined by:

$$|J| = \sqrt{(\frac{\partial y}{\partial \xi}\frac{\partial z}{\partial \eta} - \frac{\partial z}{\partial \xi}\frac{\partial y}{\partial \eta})^2 + (-\frac{\partial x}{\partial \xi}\frac{\partial z}{\partial \eta} + \frac{\partial z}{\partial \xi}\frac{\partial x}{\partial \eta})^2 + (\frac{\partial x}{\partial \xi}\frac{\partial y}{\partial \eta} - \frac{\partial y}{\partial \xi}\frac{\partial x}{\partial \eta})^2} \tag{23}$$

Derivatives with respect to local coordinates may be found by derivation of interpolation functions, i.e.

$$\begin{aligned} \frac{\partial x}{\partial \xi} &= \sum_{j=1}^4 x_j \frac{\partial \Phi_j}{\partial \xi} \qquad \frac{\partial x}{\partial \eta} = \sum_{j=1}^4 x_j \frac{\partial \Phi_j}{\partial \eta} \qquad \frac{\partial y}{\partial \xi} = \sum_{j=1}^4 y_j \frac{\partial \Phi_j}{\partial \xi} \\ \frac{\partial y}{\partial \eta} &= \sum_{j=1}^4 y_j \frac{\partial \Phi_j}{\partial \eta} \qquad \frac{\partial z}{\partial \xi} = \sum_{j=1}^4 z_j \frac{\partial \Phi_j}{\partial \xi} \qquad \frac{\partial z}{\partial \eta} = \sum_{j=1}^4 z_j \frac{\partial \Phi_j}{\partial \eta} \end{aligned} \tag{24}$$

where

$$\begin{aligned} \frac{\partial \Phi_1}{\partial \xi} &= -\frac{1}{4}(1-\eta), \qquad \frac{\partial \Phi_2}{\partial \xi} = \frac{1}{4}(1-\eta), \\ \frac{\partial \Phi_3}{\partial \xi} &= \frac{1}{4}(1+\eta), \qquad \frac{\partial \Phi_4}{\partial \xi} = -\frac{1}{4}(1+\eta), \end{aligned} \tag{25}$$

$$\begin{aligned} \frac{\partial \Phi_1}{\partial \eta} &= -\frac{1}{4}(1-\xi), \qquad \frac{\partial \Phi_2}{\partial \eta} = -\frac{1}{4}(1+\xi), \\ \frac{\partial \Phi_3}{\partial \eta} &= \frac{1}{4}(1+\xi), \qquad \frac{\partial \Phi_4}{\partial \eta} = \frac{1}{4}(1-\xi), \end{aligned} \tag{26}$$

The unit normal on the surface is calculated by

$$\vec{n} = \frac{\begin{pmatrix} \frac{\partial x}{\partial \xi} \\ \frac{\partial y}{\partial \xi} \\ \frac{\partial z}{\partial \xi} \end{pmatrix} \times \begin{pmatrix} \frac{\partial x}{\partial \eta} \\ \frac{\partial y}{\partial \eta} \\ \frac{\partial z}{\partial \eta} \end{pmatrix}}{\left| \begin{pmatrix} \frac{\partial x}{\partial \xi} \\ \frac{\partial y}{\partial \xi} \\ \frac{\partial z}{\partial \xi} \end{pmatrix} \times \begin{pmatrix} \frac{\partial x}{\partial \eta} \\ \frac{\partial y}{\partial \eta} \\ \frac{\partial z}{\partial \eta} \end{pmatrix} \right|} \tag{27}$$

When element geometry has a large aspect ratio it is necessary to divide the integral into part, which are approximately square. The integral in local coordinate system

$$\int_{-1}^{1}\int_{-1}^{1} f(\xi,\eta)d\xi d\eta, \tag{28}$$

where $f(\xi,\eta)$ is the function defined in equation (20) or (21) may be written as a sum of integrals over surfaces defined by $(a_i,b_i)\times(c_i,d_i)$

$$\int_{-1}^{1}\int_{-1}^{1} f(\xi,\eta)d\xi d\eta = \sum_i \int_{a_i}^{b_i}\int_{c_i}^{d_i} f(\xi,\eta)d\xi d\eta. \tag{29}$$

By defining new variables $(\overline{\xi},\overline{\eta})$

$$\overline{\xi} = 2\frac{\xi - a_i}{b_i - a_i} - 1 \qquad \xi = a_i + \frac{\overline{\xi}+1}{2}(b_i - a_i) \tag{30}$$

$$\overline{\eta} = 2\frac{\xi - c_i}{d_i - c_i} - 1 \qquad \xi = c_i + \frac{\overline{\xi}+1}{2}(d_i - c_i) \tag{31}$$

$$d\xi = \frac{b_i - a_i}{2}d\overline{\xi} \tag{32}$$

$$d\eta = \frac{d_i - c_i}{2}d\overline{\eta} \tag{33}$$

we obtain

$$\int_{-1}^{1}\int_{-1}^{1} f(\xi,\eta)d\xi d\eta =$$

$$\sum_i \frac{b_i - a_i}{2}\frac{d_i - c_i}{2}\int_{-1}^{1}\int_{-1}^{1} f(a_i + \frac{\overline{\xi}+1}{2}(b_i - a_i), c_i + \frac{\overline{\xi}+1}{2}(d_i - c_i))d\overline{\xi}d\overline{\eta}. \tag{34}$$

2.4 Setting up the system of equations

In each hexahedral element there are 26 function nodes on the surface (8 corners, 6 middle of surfaces and 12 on middle of edges) and 24 flux nodes (4 on each side). In order to set up a system of equations the source point is set in all of those nodes (24+26=50). Additionally, the source point is set into a node in the centre of the hexahedron, where the function value may be obtained explicitly from known boundary values. Thus all in all we have 51 equations for each element.

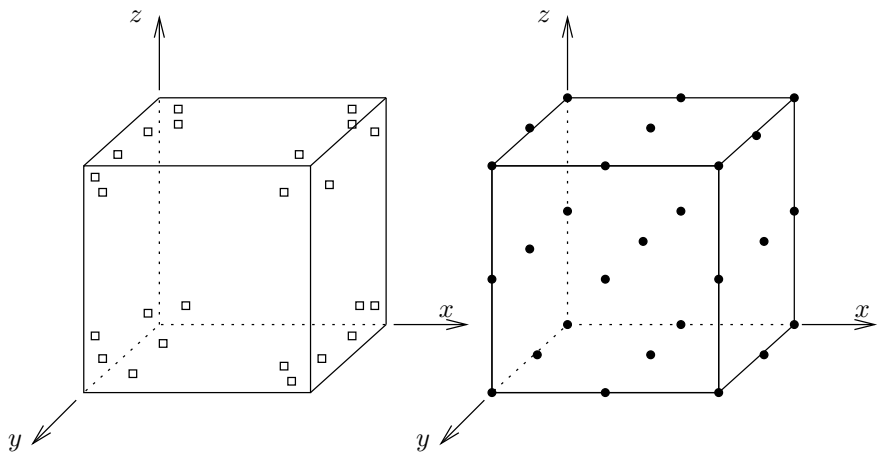

Figure 2: A hexahedron with distribution of nodes: left flux, right function

Since neighbouring elements share nodes and since boundary conditions on the outer boundaries of the domain are prescribed, we obtain an over determined system of equations. It is solved in a least squares manner.

Calculation of the free coefficient $c(\vec{\vartheta})$. When a rigid body movement is applied, $u = 1$, $q = 0$, we see that the sum of all H matrix elements for one source point must be equal to 0, thus we may use this fact to calculate $c(\vec{\vartheta})$. If the source point is located on the surface, we know that $c = 1/2$, also if the source point is inside of the element then $c = 1$. Those two are used to check the accuracy of calculated integrals.

2.5 Numerical examples

2.5.1 Heat transfer

Heat transfer over a square domain is considered. Function is prescribed on two sides, while $q = 0$ is prescribed on other four. See Figure 2.5.1 for contours of the solution.

The second example investidated was heat transfer over a cube with a cubic empty space inside. On two sides of the cube and on two sides of the empty space the function was prescribed, on all other sides adiabatic boundary condition was employed ($q = 0$). See Figure 2.5.1 for contours of the solution.

The accuracy of the calculated function and flux was compared with the analytical values. A RMS error

$$RMSerror = \sqrt{\frac{\sum_i (f_i - a_i)^2}{\sum_i a_i^2}}, \tag{35}$$

where f_i is the calculated value in node i and a_i is the analytical value in node i, was calculated. The accuracy of integration was measured using known values for the free coefficient c.

Table 1 summarizes the different meshes used. Meshes a-h were used to calculate heat transfer over a cube (left side of Figure 4) , meshes i-k were used

	mesh	domain	N_{elem}	N_{eq}	N_{unk}	nit
a	$1 \times 1 \times 1$	$(0,0,0) \times (1,1,1)$	1	51	17	6
b	$2 \times 2 \times 2$	$(0,0,0) \times (1,1,1)$	8	408	155	32
c	$2 \times 2 \times 2$	$(0,0,0) \times (1,10^{-2},1)$	8	408	155	195
d	$4 \times 4 \times 4$	$(0,0,0) \times (1,1,1)$	64	3264	1271	85
e	$4 \times 4 \times 4$	$(0,0,0) \times (1,10^{-2},1)$	64	3264	1271	1033
f	$8 \times 8 \times 8$	$(0,0,0) \times (1,1,1)$	512	26112	10223	225
g	$16 \times 16 \times 16$	$(0,0,0) \times (1,1,1)$	4096	208896	81887	436
h	$32 \times 32 \times 32$	$(0,0,0) \times (1,1,1)$	32768	1671168	655295	985
i	kvk-6	$(0,0,0) \times (3,3,3)$	6	306	106	112
j	kvk-48	$(0,0,0) \times (3,3,3)$	48	2448	934	287
k	kvk-384	$(0,0,0) \times (3,3,3)$	384	19584	7630	522

Table 1: Heat transfer test case. The function is changing linearly along the x axis. N_{elem} is the number of hexahedrons, N_{eq} is the number of equations, N_{unk} is the number of unknowns and nit is the number of iterations of the least squares solver.

for the cube in a cube numerical example (right side of Figure 4).

The main conclusion is that the accuracy of the solution depends on the accuracy of the calculation of integrals. For elements with large aspect ratio (meshes c and f), we needed to divide the integration surface in order to achieve high order of accuracy. This prolonged integration times severely.

Razlage zakaj je natancnost slaba pri mrezi kvk-48 in kvk-384 nimam. Razlika je edino v obliki heksaedrov, tu so manj podobni pravilnim kvadrom.

mesh	u source	q source	u RMS error	q RMS error
a	$2.0 \cdot 10^{-15}$	$2.0 \cdot 10^{-16}$	$1.3 \cdot 10^{-15}$	$9.4 \cdot 10^{-15}$
b	$2.0 \cdot 10^{-15}$	$2.0 \cdot 10^{-16}$	$4.0 \cdot 10^{-15}$	$1.6 \cdot 10^{-14}$
c	$1.3 \cdot 10^{-13}$	$1.2 \cdot 10^{-11}$	$1.8 \cdot 10^{-13}$	$8.1 \cdot 10^{-11}$
d	$2.0 \cdot 10^{-15}$	$2.1 \cdot 10^{-16}$	$2.6 \cdot 10^{-13}$	$1.5 \cdot 10^{-12}$
e	$1.3 \cdot 10^{-13}$	$1.3 \cdot 10^{-11}$	$1.0 \cdot 10^{-12}$	$6.3 \cdot 10^{-10}$
f	$1.9 \cdot 10^{-15}$	$2.1 \cdot 10^{-16}$	$3.4 \cdot 10^{-13}$	$9.7 \cdot 10^{-12}$
g	$1.9 \cdot 10^{-15}$	$2.7 \cdot 10^{-16}$	$8.6 \cdot 10^{-13}$	$8.3 \cdot 10^{-11}$
h	$1.9 \cdot 10^{-15}$	$1.4 \cdot 10^{-12}$	$2.6 \cdot 10^{-11}$	$2.0 \cdot 10^{-10}$
i	$2.6 \cdot 10^{-16}$	$1.1 \cdot 10^{-11}$	$3.1 \cdot 10^{-13}$	$2.9 \cdot 10^{-12}$
j	$1.7 \cdot 10^{-15}$	$4.2 \cdot 10^{-14}$	$4.5 \cdot 10^{-4}$	$2.0 \cdot 10^{-3}$
k	$1.6 \cdot 10^{-15}$	$1.5 \cdot 10^{-12}$	$3.1 \cdot 10^{-4}$	$2.5 \cdot 10^{-1}$

Table 2: Heat transfer test case. The function is changing linearly along the x axis. Error values for calculation of integrals when the source point is in u nodes and in q nodes and RMS error of function and flux.

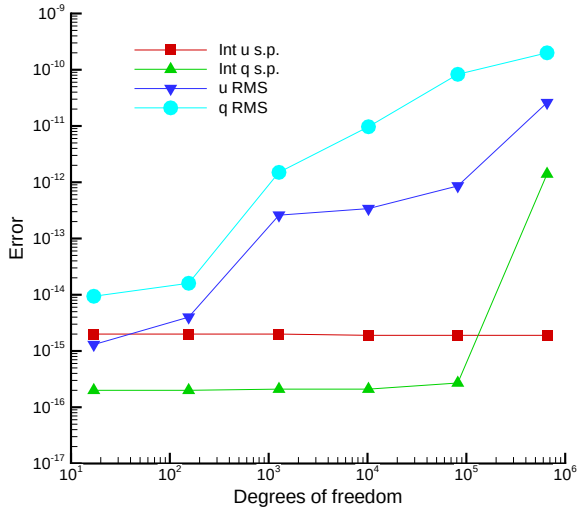

Figure 3: Dependence of function and flux RMS errors and integral calculation errors on the number of degrees of freedom.

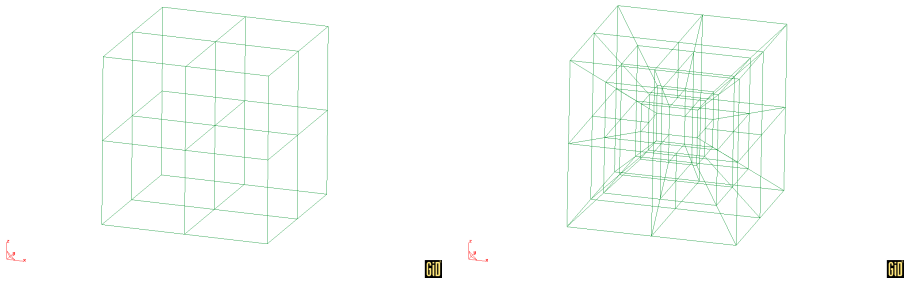

Figure 4: Meshes. Left: cube $2 \times 2 \times 2$, right: cube in a cube, 48 cells.

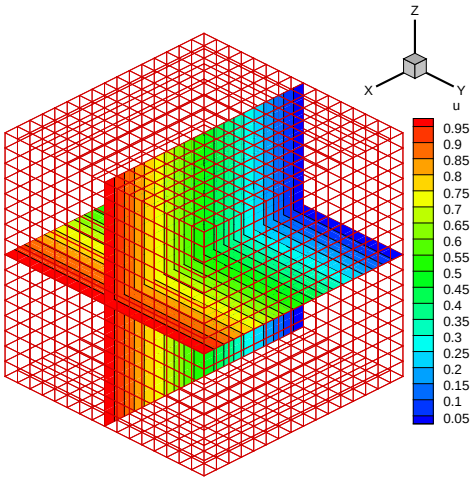

Figure 5: Heat transfer in a cube. Function on a $8 \times 8 \times 8$ mesh.

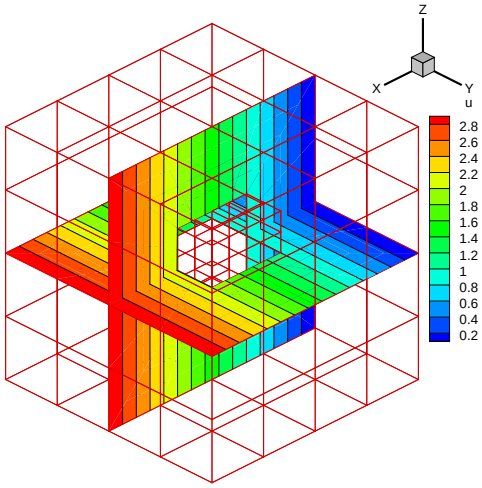

Figure 6: Heat transfer in a cube with a cube inside. Function on a 48 cell mesh.

mesh	a RMS error		b RMS error		c RMS error	
	u	q	u	q	u	q
$1 \times 1 \times 1$	$4.5 \cdot 10^{-14}$	$2.8 \cdot 10^{-14}$	$1.3 \cdot 10^{-13}$	$1.3 \cdot 10^{-3}$	$2.4 \cdot 10^{0}$	$1.9 \cdot 10^{-3}$
$2 \times 2 \times 2$	$1.3 \cdot 10^{-14}$	$2.7 \cdot 10^{-14}$	$3.6 \cdot 10^{-14}$	$3.7 \cdot 10^{-4}$	$2.1 \cdot 10^{-2}$	$1.0 \cdot 10^{-3}$
$4 \times 4 \times 4$	$4.7 \cdot 10^{-13}$	$1.3 \cdot 10^{-12}$	$1.7 \cdot 10^{-14}$	$1.0 \cdot 10^{-4}$	$1.7 \cdot 10^{-3}$	$4.4 \cdot 10^{-4}$
$8 \times 8 \times 8$	$4.7 \cdot 10^{-13}$	$6.7 \cdot 10^{-12}$	$3.4 \cdot 10^{-14}$	$2.8 \cdot 10^{-5}$	$2.9 \cdot 10^{-4}$	$1.9 \cdot 10^{-4}$
$16 \times 16 \times 16$	$2.0 \cdot 10^{-12}$	$8.6 \cdot 10^{-11}$	$4.5 \cdot 10^{-14}$	$7.4 \cdot 10^{-6}$	$6.7 \cdot 10^{-5}$	$3.7 \cdot 10^{-5}$
$32 \times 32 \times 32$	$2.5 \cdot 10^{-11}$	$1.3 \cdot 10^{-10}$	$2.5 \cdot 10^{-13}$	$1.9 \cdot 10^{-6}$	$1.6 \cdot 10^{-5}$	$9.4 \cdot 10^{-6}$

Table 3: Poisson equation.

mesh	solver iterations			solver CPU time [s]		
	a)	b)	c)	a)	b)	c)
$1 \times 1 \times 1$	6	9	7	0	0	0
$2 \times 2 \times 2$	32	36	33	0	0	0.01
$4 \times 4 \times 4$	86	109	108	0.07	0.09	0.09
$8 \times 8 \times 8$	226	279	278	2.01	2.46	2.45
$16 \times 16 \times 16$	437	894	846	33.35	68.06	64.41
$32 \times 32 \times 32$	966	2661	2409	612.58	1684.59	1515.99

Table 4: Poisson equation - B.

3 Poisson equation

Numerical examples

a) equation $\nabla^2 u = 2$, analytical solution $u = x^2$, boundary conditions $u(0, y, z) = 0$, $u(1, y, z) = 1$, $q(x, 0, z) = q(x, 1, z) = q(x, y, 0) = q(x, y, 1) = 0$.

b) equation $\nabla^2 u = 6x$, analytical solution $u = x^3$, boundary conditions $u(0, y, z) = 0$, $u(1, y, z) = 1$, $q(x, 0, z) = q(x, 1, z) = q(x, y, 0) = q(x, y, 1) = 0$.

c) equation $\nabla^2 u = 12x^2$, analytical solution $u = x^4$, boundary conditions $u(0, y, z) = 0$, $u(1, y, z) = 1$, $q(x, 0, z) = q(x, 1, z) = q(x, y, 0) = q(x, y, 1) = 0$.

4 Diffusion advection equation

entry flow

5 vorticity transport eqaution equation

The domain integral, which includes advection and wortex twisting and streatching terms is

$$\int_{\Omega} \left\{ (\vec{\omega} \cdot \vec{\nabla})\vec{v} - (\vec{v} \cdot \vec{\nabla})\vec{\omega} \right\} u^* d\Omega \tag{36}$$

Lets consider only the j component of the vector eqaution (36)

$$\int_{\Omega} \left\{ (\vec{\omega} \cdot \vec{\nabla})v_j - (\vec{v} \cdot \vec{\nabla})\omega_j \right\} u^* d\Omega \tag{37}$$

Due to the solenidality of the veloctiy and vorticity fields, we may write

$$(\vec{\omega} \cdot \vec{\nabla})v_j = \vec{\nabla} \cdot (\vec{\omega} v_j) \qquad (\vec{v} \cdot \vec{\nabla})\omega_j = \vec{\nabla} \cdot (\vec{v}\omega_j) \tag{38}$$

Using (38) in (37) we have

$$\int_{\Omega} \left\{ \vec{\nabla} \cdot (\vec{\omega} v_j - \vec{v}\omega_j) \right\} u^* d\Omega \tag{39}$$

In order to move the derivetive towards the fundamental solution, the following algebraic relation come in handy

$$\vec{\nabla} \cdot \{u^*(\vec{\omega} v_j - \vec{v}\omega_j)\} = u^* \vec{\nabla} \cdot (\vec{\omega} v_j - \vec{v}\omega_j) + (\vec{\omega} v_j - \vec{v}\omega_j) \cdot \vec{\nabla} u^* \tag{40}$$

Using (40) in (39) we obtain two integrals

$$\int_{\Omega} \vec{\nabla} \cdot \{u^*(\vec{\omega} v_j - \vec{v}\omega_j)\} \, d\Omega - \int_{\Omega} (\vec{\omega} v_j - \vec{v}\omega_j) \cdot \vec{\nabla} u^* d\Omega \tag{41}$$

The first integral may be converted to a boundary integral using a Gauss divergence clause, thus

$$\int_{\Gamma} \vec{n} \cdot \{u^*(\vec{\omega} v_j - \vec{v}\omega_j)\} \, d\Gamma - \int_{\Omega} (\vec{\omega} v_j - \vec{v}\omega_j) \cdot \vec{\nabla} u^* d\Omega \tag{42}$$

The products of velocity and vorticity field components are interpolated within elements by

$$(v_i \omega_j) = \sum_l \varphi_l (v_i \omega_j)_l \qquad (v_i \omega_j) = \sum_l \varphi_l^d (v_i \omega_j)_l \tag{43}$$

where φ^d are 27 domain shape functions.

$$\begin{aligned}
&\left\{ \sum_l (v_x \omega_j)_l - \sum_l (v_j \omega_x)_l \right\} \left\{ \int_{\Gamma} n_x \varphi_l d\Gamma - \int_{\Omega} \frac{\partial u^*}{\partial x} \varphi_l^d d\Omega \right\} \\
+ &\left\{ \sum_l (v_y \omega_j)_l - \sum_l (v_j \omega_y)_l \right\} \left\{ \int_{\Gamma} n_y \varphi_l d\Gamma - \int_{\Omega} \frac{\partial u^*}{\partial z} \varphi_l^d d\Omega \right\} \\
+ &\left\{ \sum_l (v_z \omega_j)_l - \sum_l (v_j \omega_z)_l \right\} \left\{ \int_{\Gamma} n_z \varphi_l d\Gamma - \int_{\Omega} \frac{\partial u^*}{\partial y} \varphi_l^d d\Omega \right\}
\end{aligned} \tag{44}$$

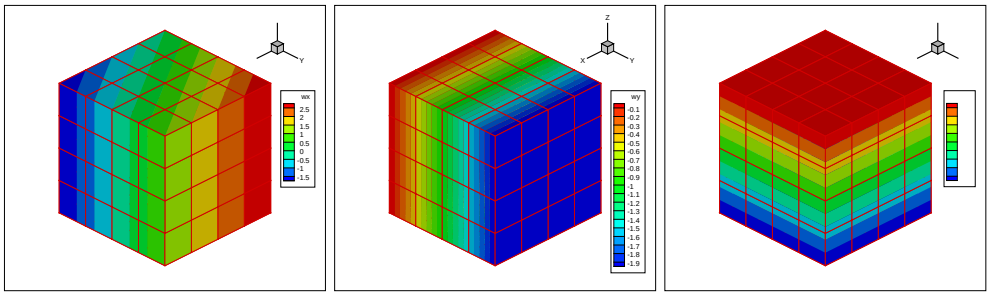

Figure 7: Vorticity.

With this, when the matrices are formed, we may sum up the boudnary and domain integral values. Thus we require only three matrices of integrals for both advective and twisting and stretching terms.

By prescribing the following veloctiy field $\vec{v} = (yz, 2xz, 3xy)$ and boundary vorticity values $\vec{\omega} = (-2x + 3y, -2y, z)$, we were able to check the vorticity transport eqaution. The results obtained were analytical for all three vorcitiy components on every mesh tries, including the $1 \times 1 \times 1$ mesh.

5.1 Couette X

$\vec{v} = (z, 0, 0)$, $\vec{\omega} = (0, 1, 0)$ inflow $x = 0$, outflow $x = 1$, top $z = 1$, bottom $z = 0$, symmetry walls $y = 0$, $y = 1$

Velocity boundary conditions:

v_x inflow and top and bottom walls $v_x = z$, outflow and symetry walls $\partial v_x / \partial n = 0$

v_y all walls $v_y = 0$

v_z inflow and top and bottom walls $v_z = 0$, outflow and symetry walls $\partial v_z / \partial n = 0$

Vorticity boundary conditions:

ω_x all walls $\omega_x = 0$

ω_y inflow and top and bottom walls $\omega_y = km$, outflow and symetry walls $\partial \omega_y / \partial n = 0$

ω_z all walls $\omega_z = 0$

5.2 Couette Y

$\vec{v} = (0, x, 0)$, $\vec{\omega} = (0, 0, 1)$ inflow $y = 0$, outflow $y = 1$, top $x = 1$, bottom $x = 0$, symmetry walls $z = 0$, $z = 1$

Velocity boundary conditions:

v_x inflow and top and bottom walls $v_x = 0$, outflow and symetry walls $\partial v_x / \partial n = 0$

v_y inflow and top and bottom walls $v_y = x$, outflow and symetry walls $\partial v_y/\partial n = 0$

v_z all walls $v_z = 0$

Vorticity boundary conditions:

ω_x all walls $\omega_x = 0$

ω_y all walls $\omega_y = 0$

ω_z inflow and top and bottom walls $\omega_z = km$, outflow and symetry walls $\partial \omega_z/\partial n = 0$

5.3 Couette Z

$\vec{v} = (0, 0, y)$, $\vec{\omega} = (1, 0, 0)$ inflow $z = 0$, outflow $z = 1$, top $y = 1$, bottom $y = 0$, symmetry walls $x = 0$, $x = 1$

Velocity boundary conditions:

v_x all walls $v_x = 0$

v_y inflow and top and bottom walls $v_y = x$, outflow and symetry walls $\partial v_y/\partial n = 0$

v_z inflow and top and bottom walls $v_z = 0$, outflow and symetry walls $\partial v_z/\partial n = 0$

Vorticity boundary conditions:

ω_x inflow and top and bottom walls $\omega_x = km$, outflow and symetry walls $\partial \omega_x/\partial n = 0$

ω_y all walls $\omega_y = 0$

ω_z all walls $\omega_z = 0$

References

[1] J. Ravnik. *Metoda robnih elementov za hitrostno vrtinčno formulacijo simulacije velikih vrtincev.* PhD thesis, Univerza v Mariboru, Fakulteta za strojništvo, 2006.

[2] L. C. Wrobel. *The Boundary Element Method.* John Willey & Sons, LTD, 2002.